

Energy Confinement and Heat Transport in Extended High Density Regime of NBI Heated Plasmas on LHD

H.Yamada, S.Murakami, R.Sakamoto, J.Miyazawa, S.Morita, K.Y.Watanabe, K.Narihara,
K.Tanaka, S.Sakakibara, B.J.Peterson, K.Ida, M.Osakabe, S.Inagaki, S.Masuzaki,
G.Rewoldt¹, H.Sugama, O.Kaneko, K.Kawahata, A.Komori, Y.Nakamura, T.Mutoh,
N.Ohyabu, K.Yamazaki, O.Motojima, LHD Experimental Group

*National Institute for Fusion Science, Toki, Gifu 509-5292, Japan
1 Princeton Plasma Physics Laboratory, Princeton, NJ 08544, USA*

1.Introduction

Confinement studies of net current free plasmas have progressed due to the recent LHD experiments with upgraded heating capability up to 9 MW of NBI. Significant density dependence of the energy confinement time as described in the ISS95 scaling [1] has been demonstrated [2,3] in the extended parameter regimes in LHD. When the plasma profiles are fixed, the density dependence of the energy confinement time, i.e., $\tau_E \propto (\bar{n}_e / P)^{0.6}$ or $\tau_E \propto (\bar{n}_e / P)^{0.5}$ can be interpreted by the gyro-Bohm local heat conduction as $\chi \propto T^{3/2}$ or the Bohm as $\chi \propto T$, respectively. The favorable density dependence observed in LHD is of importance with the prospect of net current-free plasmas with high confinement and high β due to high density operation. Since the density dependence of the global confinement and the temperature dependence of the local transport are two sides of the same physical mechanism, it is also attracting much interest to the physics issue of anomalous transport. However, the existence of this kind of density dependence and its disappearance have been reported from many toroidal experiments. Recent experiments employing a wide range of heating power in LHD also have indicated that the favorable density dependence saturates at

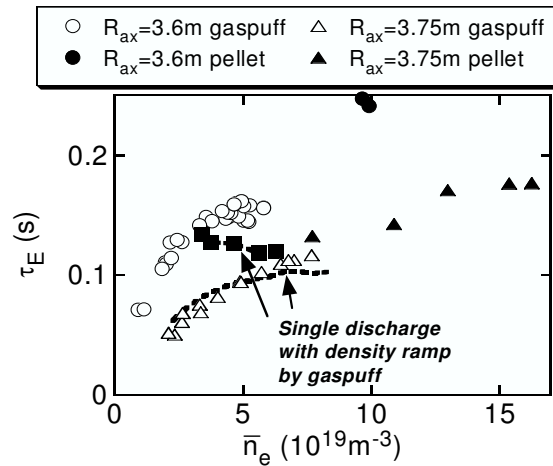


Fig.1 Dependence of energy confinement time on density in the density scan with fixed heating power. Open and Solid symbols denote gas-fueled and pellet-fueled discharges, respectively. Circles and triangles are the cases with $R_{ax}=3.6$ m and 3.75 m, respectively. Dashed lines : time traces of single discharges with density ramp-up. The heating power is fixed at 4.5 MW and 3.6 MW in the cases with $R_{ax}=3.6$ m and $R_{ax}=3.75$ m, respectively.

a certain density under specific conditions. This paper discusses the cause of this saturation and related characteristics of anomalous transport. Through this study, the response of temperature profile to the heat deposition profile is highlighted, which is contrasted to the concept of *stiffness* or *profile consistency* observed in tokamaks.

2. Experimental Results

Although confinement improvement by shifting the magnetic axis inward has been demonstrated in previous work [2], saturation of the energy confinement time with the increase in density has been observed in gas-fueled NBI-heated plasmas, particularly, with this inward shifted configuration with $R_{ax}=3.6$ m. Open circles in Fig.1 shows the data in the density flat phase for a series of density scan with the fixed heating power of 4.5MW in the case with $R_{ax}=3.6$ m. The energy confinement time does not increase anymore above $4 \times 10^{19} \text{m}^{-3}$. The energy confinement time is derived from the stored energy measured by the diamagnetic loop and the absorbed heating power estimated from the direct measurement of the shine-through power [4] and the Monte-Carlo calculation [5]. Excess gas-puffing to increase density shrinks the plasma and consequently degrades the performance; however, the saturation of the energy confinement has been found well below this condition. The saturated state can be sustained in a quasi-steady state and radiation loss does not play an essential role. The saturation density does not depend on the heating power significantly and shows a weak dependence on the magnetic field strength. The saturation or degradation of confinement is distinguished in the density ramp-up phase by gas-puffing in a single discharge with $R_{ax}=3.6$ m. The discharge shown in Fig.2 corresponds to the closed squares in Fig.1 with time slices every 0.5s. The line averaged density is doubled from $t = 1.5$ s to 4.0 s, however, the stored energy and the energy confinement time do not change.

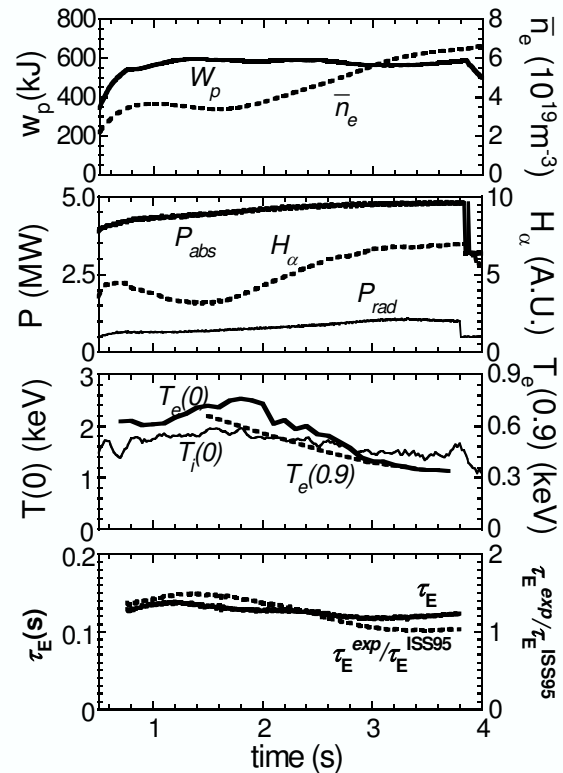


Fig.2 Waveforms of the discharge with density ramp-up. The working gas is hydrogen. Top: Stored energy and line averaged density. 2nd: Absorbed power of NBI, total radiation power, and $H\alpha$ emission. 3rd: The electron temperatures at the center and $\rho=0.9$ measured by the multi-channel Thomson scattering system, and the ion temperatures measured by the crystal spectrometer (Ti XXI). Bottom: Energy confinement time and improvement factor on ISS95.

The saturation density does not depend on the heating power significantly and shows a weak dependence on the magnetic field strength. The saturation or degradation of confinement is distinguished in the density ramp-up phase by gas-puffing in a single discharge with $R_{ax}=3.6$ m. The discharge shown in Fig.2 corresponds to the closed squares in Fig.1 with time slices every 0.5s. The line averaged density is doubled from $t = 1.5$ s to 4.0 s, however, the stored energy and the energy confinement time do not change.

The improvement factor on ISS95 is degraded from 1.6 to 1. The ratio of the radiation power to the absorbed power increases from 16 % to 22 %. Although temperatures decrease with the increase in density, the ratio of decrease of electron temperature is more distinguished in the center than in the edge. Ion temperature is reduced more gradually because of stronger equi-partition of energy with electrons in the higher density regime. The temporal changes of the density and temperature profiles are shown in Fig.3. The density profile remains flat during the ramp-up and the electron temperature becomes broad.

The high density operation prevents the deep penetration of tangentially injected neutral beams and heat deposition moves from the core to the periphery (see Fig.4(a)). This tendency is emphasized with

the inward-shifted magnetic axis due to the tangent radius of 3.7 m of the NBI beam lines and the broad density profile due to gas-puffing particularly in the ramp-up phase. The local heat transport is investigated for time slices in the density ramp-up phase with $R_{ax}=3.6\text{m}$. Although the density dependence going as $\tau_E \propto \bar{n}_e^{0.6}$ is lost completely, the local heat conduction coefficient shows a clear temperature dependence with the power of 1.0 to 1.6 (see Fig.4(b)). Although the discussion whether Bohm or gyro-Bohm it is requires clarification of the dependence on the magnetic field strength, the essential point is that the apparent contradiction between the global confinement and the local transport can be attributed to the change of the heat deposition profile.

In contrast to the case with $R_{ax}=3.6\text{m}$, the density dependence of gas-fueled plasmas is sustained in the high density regime close to the detachment of the plasma in the case with $R_{ax}=3.75\text{m}$ (see triangles in Fig.1). The degradation due to the density ramp-up is not so distinguished as in $R_{ax}=3.6\text{m}$. The heat deposition profile is insensitive to density itself as

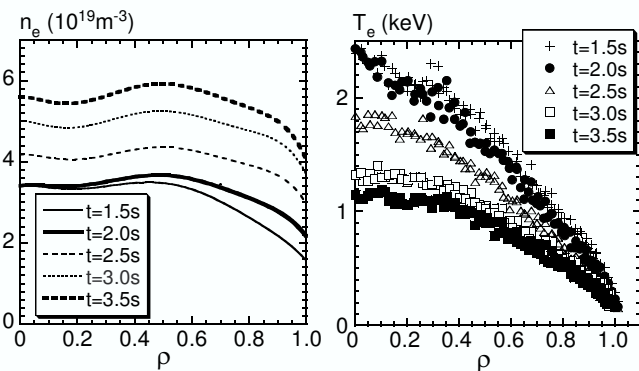


Fig.3 Left (a): Temporal change of density profile in the discharge with $R_{ax}=3.6\text{ m}$ illustrated in Fig.2. Right (b): Temporal change of temperature profile.

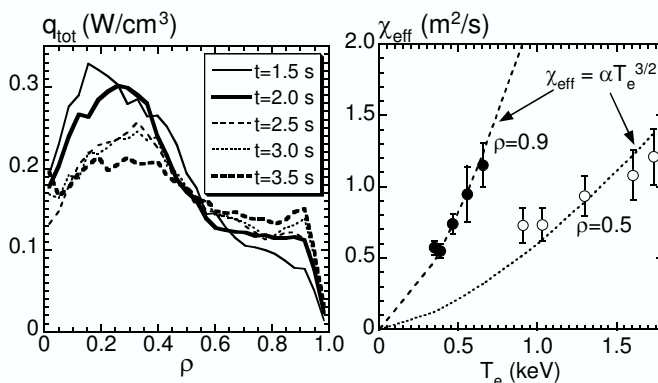


Fig.4 Left (a) : Profile of power deposition from NBI in the discharge illustrated in Fig.2 with $R_{ax}=3.6\text{m}$. Right (b) : Temperature dependence of thermal diffusivity at two radii of $\rho=0.5$ (open circles) and $\rho=0.9$ (solid circles) derived from the power balance analysis of 5 time slices.

well as its profile (see Fig.5(a)) in this case. The thermal diffusivity shows a clear the temperature dependence as in the case with $R_{ax}=3.6\text{m}$, which is consistent with the behavior of the energy confinement time because of the unchanged heat deposition profile.

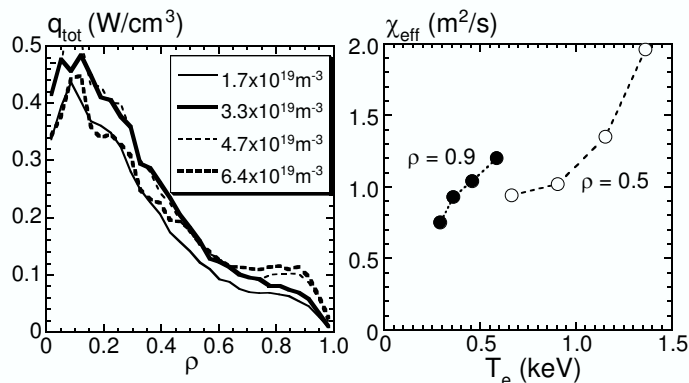


Fig.5 Left (a) : Profile of power deposition from NBI in the discharges in the case with $R_{ax}=3.75\text{m}$. Right (b) : Temperature dependence of thermal diffusivity at two radii of $\rho=0.5$ (open circles) and $\rho=0.9$ (solid circles) derived from the power balance.

3. Discussions and Conclusions

Major part of an apparent contradiction between the global energy confinement time and local thermal diffusivity, which has been observed in the case with $R_{ax}=3.6\text{m}$, can be explained by the broadening of heat deposition. These observations indicate that the temperature profile changes straight-forwardly according to the heat deposition profile of the net current free plasmas in LHD. The apparent discrepancy between the global and the local transports suggests that the central heating improves the saturated state. The favorable density dependence can be extended towards much higher density by pellet fueling (see closed circles and triangles in Fig.1)[6] in both cases of $R_{ax}=3.6\text{ m}$ and 3.75 m . The peaked density profile realized by pellet fueling promotes the core heating and recovers the intrinsic density dependence when the density is moderate. However, the peripheral heat deposition becomes predominant even in the peaked density profile by pellet injection above $8 \times 10^{19}\text{m}^{-3}$, therefore, other mechanism related to confinement improvement is prerequisite to explain the advantage of pellet injection.

References

- [1] U.Stroth, M.Murakami, H.Yamada *et al.*, Nucl. Fusion **36** (1996) 1063.
- [2] H.Yamada, K.Y.Watanabe, K.Yamazaki *et al.*, Nucl. Fusion **41** (2001) 901.
- [3] H.Yamada, A.Komori, N.Ohyabu *et al.*, Plasma. Phys. Control. Fusion **43** (2001) A55.
- [4] M.Osakabe *et al.*, Rev. Sci. Instrum. **72**, 590 (2001)
- [5] S.Murakami *et al* 1995 *Trans. Fusion Technol.* **27** (1995) 256
- [6] R.Sakamoto, H.Yamada, K.Tanaka *et al.*, Nucl. Fusion **41** (2001)381.